LAWRENCE
LIVERMORE
NATIONAL
LABORATORY

UCRL-JRNL-235324

Spin-Orbit Effects in Spin-Resolved L2,3 Core Level Photoemission of 3d Ferromagnetic Thin Films

T. Komesu, G. D. Waddill, S. W. Yu, M. Butterfield, J. G. Tobin

October 5, 2007

Journal of Vacuum Science and Technology A

Updated October 14, 2003

Spin-Orbit Effects in Spin-Resolved $L_{2,3}$ Core Level Photoemission of 3d Ferromagnetic Thin Films

T. Komesu*, G.D. Waddill,

University of Missouri-Rolla, Department of Physics, Rolla, MO 65401-0249

S.-W. Yu, M. Butterfield, and J.G. Tobin

Lawrence Livermore National Laboratory, Livermore, CA 94550

Abstract:

We present spin-resolved 2p core level photoemission for the 3d transition metal films of Fe and Co grown on Cu(100). We observe clear spin asymmetry in the main 2p core level photoemission peaks of Fe and Co films consistent with trends in the bulk magnetic moments. The spin polarization can be strongly enhanced, by variation of the experimental geometry, when the photoemission is undertaken with circularly polarized light, indicating that spin-orbit interaction can have a profound in spin polarized photoemission. Further spin polarized photoemission studies using variable circularly polarized light at high photon energies, high flux are indicated, underscoring the value of synchrotron measurements at facilities with increased beam stability.

PACS numbers

Keywords: spin resolved photoemission, spin orbital effect, exchange effect, core level, transition metal

*Present address: Spring8, Japan

The spin-polarized photoemission from core levels is strongly dependent upon two different and completing effects: exchange splitting and spin orbit splitting. [1] In fact, it is possible to observe strongly spin polarized photoemission from completely "non-magnetic" systems. [2] Here, using circularly polarized x-rays and true spin detection, this interplay and competition will be quantified.

Transition metals of single crystal thin films have been widely characterized with spin resolved photoelectron spectroscopy (SRPES) at the 2p ($L_{2,3}$-edge) core levels [3-5]. Some of the magnetic transition 3d metals exhibit quite complex core level spectra, as in the case of the correlated electron metal Ni [6]. Although there are indications of a satellite in Co, as can be seen below in Figure 1, a detailed analysis of that topic will be left for a future publication. Instead, here the focus will be upon the interplay of exchange and spin-orbit effects in Fe 2p and Co 2p spin polarized photoemission. (Figure 1) In this letter, we report on the investigation of the 2p core level peaks of Fe and Co films grown on Cu(100), using spin resolved photoelectron spectroscopy (SRPES). Circularly polarized x-rays were provided at Advanced Photon Source by the Sector 4 Elliptically Polarizing Undulator (EPU). We compare these results with detailed spectral simulations (Figure 2) based upon a simple yet effective model [1] that all of the essential physics of the experiment.

The key features of our spin-resolved photoemission spectroscopic experiment (Figure 3) have been previously described [7]. The photo-excited electrons are collected in a hemispherical electron energy analyzer (Physical Electronics Model 3057) with multichannel electron detection. In the Mini-Mott, spin polarized electron detector, the electrons are accelerated to ~25 kV, with four channeltrons positioned horizontally and

vertically used for electron counting. For the measurements described here, the incident angle was 55 degrees off the surface normal (in the yz plane) and the photoelectrons were collected at normal emission. All magnetic SRPES measurements were made in remanance, with the absence of an applied field during the SRPES data collection.

Thin films of ferromagnetic elements were grown on Cu(100) in previous studies [2, 8, 9]. The Cu crystal was cleaned with Ar^+ sputtering followed by annealing to about 450 °C. The films exhibited a p(1x1) LEED pattern and no observable contamination as judged from X-ray Photoemission Spectroscopy (XPS) measurements. The focus is on in-plane magnetism in 20 ML Fe and 10 ML Co films. The magnetic character of the films of Fe and Co was confirmed using x-ray magnetic circular dichroism in x-ray absorption spectroscopy (XMCD-XAS, Figure 2) [10], acquired using beamline 4ID-C at the Advanced Photon Source at Argonne National Laboratory [11]. The sample was magnetized parallel and antiparallel to the (100) or x direction in Figure 3 for Fe and Co, between successive core region spectra, using a pulsed magnetic field applied for exchange effect measurement (Figure 1), with fixed photon polarization (helicity) of the circular polarized beam. Looking at the data averaged over both magnetization directions in Figure 1, majority (minority) features are denoted as parallel (antiparallel) to the applied magnetic field, indicated with blue (red) line. With this geometry of spin resolved data acquisition (spin polarization along Px in Figure 3), it is hypothesized that the spin-orbital-driven effects will tend to cancel out each other, because of the flipping of the magnetic moment direction in the sample, with the helicity of the photon beam kept constant. With an up direction of external magnetic field, spin up state electrons (majority state) go to one channeltron after Mott scattering (R), denoted as UR, and the

spin down state electrons (minority state) go to the other channeltron (L) and denoted as UL. On the other hand, with the reverse direction (down) of the applied external magnetic field, spin down (majority state) electrons go to the other channeltron (L), denoted as DL, and spin up electrons (minority state) go to channeltron R, and denoted as DR, based on Mott detector scattering [12]. This reversal can be seen in the magnetization specific Fe spin spectra in Figure 1. Depending upon the external magnetic field, majority (minority) state electrons are collected into two channeltrons and added up with each other: UR + DL (DR + UL) for the majority (minority) state electrons. The success of this cancellation can be seen in the magnetization specific asymmetries and instrumental asymmetry plots for Fe in Figure 1.

First, consider the asymmetry, which is simply defined as the following.

A = [counts(R) – counts(L)]/[counts(R) + counts(L)] **Eq 1**

As can be sen for Fe, the asymmetry flips almost perfectly with magnetization. The effect of this is to produce a cancellation in the instrumental asymmetry (IA, eq 2), where it is a constant and near a value of 1.1.

$IA = \{[counts(UR) * counts(DR)]/[counts(DL) * counts(UR)]\}^{1/2}$ **Eq 2**

Thus, the Fe 2p results strongly confirm the hypothesis of cancellation. Conversely, the same can not be said for the Co results. Here, the asymmetry does not flip with magnetization reversal but instead is almost the same for both magnetizations. This is reflected in the signature in the Co IA, where the value is not constant. Interestingly, there is good cancellation in the polarization for both Fe and Co: the polarizations oscillate about zero. As will be shown below, these results are an indication of the

dominance of magnetic effects over Fano effects in Fe, but a weakening of the dominance in Co.

In order to understand what is going on here, it is necessary to perform spectral simulations that include all of the essential physics. Here, a model developed earlier [1] will be extended and improved. The key points are as follows. (1) The axis of quantization is along the magnetization direction. (When the magnetization flips, the coordinate system flips too.) (2) The initial states are the analytically derived, orthogonal one-electron states for the given values of exchange and spin-orbit splitting. (3) Only electric dipole transitions are allowed, with pure circular polarization along the incident direction (55 degrees from the the surface normal) being projected onto the coordinate system defined by the magnetization direction. (4) The final state is a real plane wave state, which devolves into a pure d ($l = 2$, $m = 0$) spherical harmonic, along the emission direction. Using Euler angles and the addition theorem for spherical harmonics, this state is projected onto the coordinate systems defined by the magnetization directions. (At these kinetic energies, electric dipole allowed transitions into allowed s-wave components will be insignificant compared to the d-wave component. The s-wave is thus neglected here. [1]) A summary of the states and intensities is given in Table 1. These intensities are then enwrapped in Doniach-Sunjic line-shapes [1] and summed. The results of that operation are shown in Figure 2 for Fe and Co. The spin-orbit splitting values were extracted form the literature [13] and the other parameters obtained by matching to the experimental Fe spectra. For Co, the exchange value was arrived at by scaling to the Fe exchange value via the known values of the Fe and Co magnetic moments. [14] Peak lifetime broadening varies linearly with the energy, to reflect the

well known increase in broadening between the 2p3/2 and 2p1/2 peaks. [2] The simulated spectra reconstruct all of the features of the Fe and Co, save one: only the small, high binding energy should of the Co is missing. This feature, potentially associated with electron correlation as in Ni, will be the subject of another, future publication. Interestingly, for this configuration and within this model, there is no circular polarization effect. The intensities are the same as those for unpolarized radiation. That is because the helicity (in the yz plane) is perpendicular to the axes of quantization associated with the magnetization (along plus or minus x). Also shown in Figure 2 is the ratio of the two spectra. Now, let us consider a case of incomplete magnetization.

Consider now a limiting case. Suppose that internally, each atom was magnetically polarized, but externally, all were free to rotate. Then the instrumental asymmetry (IA) would devolve into something akin to an MXLD-like result. [1] This is because now the coordinate axes are not defined by magnetization but instead by the potentially chiral configuration of the linear vectors in the experiment, such as the Poynting vector of the radiation and the emission direction of the electrons. The cross product, of these vectors, produce an axis of quantization along x, that can only be reversed by completely reconfiguring the experiment in a reverse chirality. Under these conditions equation 2 collapses to something simpler, shown in equation 3.

$$\mathbf{(IA)_{Free} = \{counts(R)/counts(L)\}^{1/2}} \qquad \mathbf{Eq\ 3}$$

This result has been plotted in Figure 2. It turns out that this is simply equivalent to the ratio of the spin specific spectra shown in Figure 2. Comparing the ratio of the spectra to the Instrumental Asymmetry of Co shown in Figure 1, it is clear that we can explain the unusaul IA for Co. The ramifications for this result is the following: Co is much less well

magnetically aligned than Fe. In Fe, the magnetization driven effects dominate. In Co, this dominance is beginning to break down and a Fano-like effect is becoming important. To test this conclusion, another spin resolved experiment, in a different geometry, was performed. This Fano measurement will be described below.

Measurement of the spin-orbital-driven Fano effect (Figure 2), was performed with a non-magnetized condition for the Co film. Here, the photon helicity of the circular polarized light was switched each scan, which should tend to cancel out contributions from the exchange effect (magnetic character from exchange interaction). Data collected with one helicity scan data were compared to data collected with the other helicity, in a manner similar to the data collection process for the exchange effect. Here, however, the helicity is flipped and the macroscopic magnetization kept constant at zero. The measurements were carried out at room temperature. These spin resolved photoemission spectra of Co grown on Cu(100) are shown in Figure 3. It is clear that there is a strong dichroic effect. Moreover, it is possible to simulate this result with a slight modification of the theory described above.

Overall, the geometry of the experimant is much the same as that for the magnetization experiments. However, now the spin being measured is along the emission direction (+/- z) , not perpendicular to it (+/-x). Additionally, the new axis of quantization is along the propagation direction of the x-rays: the coordinate system is flipped by reversing the helicity. Because of this geometry, with a co-alignment of helicity and the axes of quantization, dichroic (Fano) effects will be allowed and are expected to be very strong. The theoretical results for this geometry are shown in Table 1 and the simulated spectra are plotted in Figure 3. Obviously, the simulations reconstruct

the experimental observations, confirming that there is a strong Fano effect in Co, despite the presence of internal magnetic polarization.

Spin-orbital-driven Fano effects lead to strong spin asymmetries but with a dependence that is different than that due to the magnetization and the associated magnetic spin asymmetry. Because of Fresnel boundary conditions, a systematic study with variable circular polarization is indicated, but the trend of the spin-orbital interaction is clear. Such studies are now possible because of improvements at synchrotron light sources and associated beamlines as spin-resolved photoemission spectroscopy (SRPES) can be increasingly can be undertaken using with polarized light at photon higher energies, with excellent flux stability.

Acknowledgments

This work was performed under the auspices of the U.S. Department of Energy, by the University of California Lawrence Livermore National Laboratory under contract W-7405-Eng-48. Work that was performed by LLNL and UMR personnel was supported by the Office of Basic Energy Science at the U.S Department of Energy. The APS has been built and operated under funding from the Office of Basic Energy Science at DOE. We would like to thank the scientific and technical staff of Sector 4 of the Advanced Photon Source for their technical assistance in supporting this work. TK would like to thank Prof. Peter A. Dowben at University of Nebraska-Lincoln for valuable scientific discussions.

References

[1] J.G. Tobin and F.O. Schumann, Surface Science **478**, 211 (2001).

[2] S.W. Yu, T. Komesu, B.W. Chung, G.D. Waddill, S.A. Morton, and J.G. Tobin, Phys. Rev. B **73**, 075116 (2006).

[3] D. G. van Campen, R. J. Pouliot, and L. E. Klebanoff, Phys. Rev. B **48**, 17533 (1993)

[4] F. U. Hillebrecht, Ch. Roth, H. B. Rose, W. G. Park, E. Kisker, and N. A. Cherepkov, Phys. Rev. B **53**, 12182 (1996)

[5] C. M. Schnieder, U. Pracht, W. Kuch, A. Chassé, and J. Kirshner, Phys. Rev. B **54**, R15618 (1996)

[6] A. K. See and L. E. Klebanoff, Phys. Rev. B **51**, 11002 (1994), Phys. Rev. Lett. **74**, 1454 (1994)

[7] J.G. Tobin, S.A. Morton, S.W. Yu, T. Komesu, G.D. Waddill and P. Boyd, Nucl. Instrum. Methods, 2007, in press; J.G. Tobin, P.J. Bedrossian, T.R. Cummins, G.D. Waddill, S. Mishra, P. Larson, R. Negri, M. Miller, E. Peterson, P. Boyd, and R. Gunion, Mat. Res. Soc. Symp. Proc. **524**, 185 (1998).

[8] F. Ciccacci, S. De Rossi, Phys. Rev. B **51**, 11538 (1995)

[9] D.P. Pappas, C.R. Brundle, and H. Hopster, Phys. Rev. B **45**, 8169 (1992)

[10] J. Tobin, G. Waddill and D. Pappas, Phys. Rev. Lett. **68**, 3642 (1992); J.G. Tobin, K.W. Goodman, G.J. Mankey, R.F. Willis, J.D. Denlinger, E. Rotenberg, and A. Warwick, J. Vac. Sci. Tech., B **14**, 3171 (1996); S.Z. Wu, F.O. Schumann, R.F. Willis, K.W. Goodman, J.G. Tobin, and R. Carr, J. Vac. Sci. Tech. **A15**, 2287 (1997).

[11] J.W. Freeland, J.C. Lang, G. Srajer, R. Winarski, D. Shu, and D.M. Mills, Rev. Sci. Instrum. **73**, 1408 (2002).

[12] T. J. Gay, and F. B. Dunning, Rev. Sci. Instrum. **63**, 1635 (1992)

[13] X-ray Data Handbook, A. Thompson et al, LBNL, Jan 2001.

[14] J.G. Tobin, G.D. Waddill, E. Tamura, P. Sterne, P.J. Bedrossian, D.P. Pappas, X. Guo, and S.Y. Tong, Surf. Rev. Lett. **3**, 1429 (June 1996).

Figure captions

Figure 1 Spin resolved photoelectron spectra (SRPES) of macroscopically magnetized Fe and Co films. Here, the axis of quantization is along the +/- x direction, following the magnetization. See text for details.

Figure 2 Spectral simulations corresponding the SRPES experimental results in Figure 1 are shown here in blue and red. The ratio of the spin resolved spectra is shown in black. X-ray magnetic circular dichroism – x-ray absorption spectra (XMCD-XAS) results are shown in the inset. See text for details.

Figure 3 The experimental layout is shown in the topmost panel. The Co Fano experimental result is shown in the middle panel and the corresponding spectral simulation is shown in the lowest panel. See text for details.

Table 1

	Magnetization Experiment	Fano Experiment (RCP vs LCP)	
State	Intensity (RCP or LCP)	Intensity (RCP)	Intensity(LCP)
1,↑	1	1	~ 0
1,↓	0	0	0
2,↑	$B_1 \cos^2\theta$	$B_2 \cos^2\theta$	$B_2 \cos^2\theta$
2,↓	$\sin^2\theta$	$\sin^2\theta$	~ 0
3,↑	$\cos^2\phi$	~ 0	$\cos^2\phi$
3,↓	$B_1 \sin^2\phi$	$B_2 \sin^2\phi$	$B_2 \sin^2\phi$
4,↑	0	0	0
4,↓	1	~ 0	1
5,↑	$\sin^2\phi$	~ 0	$\sin^2\phi$
5,↓	$B_1 \cos^2\phi$	$B_2 \cos^2\phi$	$B_2 \cos^2\phi$
6,↑	$B_1 \sin^2\theta$	$B_2 \sin^2\theta$	$B_2 \sin^2\theta$
6,↓	$\cos^2\theta$	$\cos^2\theta$	~ 0
$B_1 = 4/\{5[1-(3/5)\cos 2\alpha]\}$ $B_1 \approx 0.664$ ($\alpha = 55$ degrees)		$B_2 = 2(\cos\alpha/\sin\alpha)^2$ $B_1 \approx 0.98$ ($\alpha = 55$ degrees) $\sim 0 \rightarrow 0$ as $\alpha \rightarrow 54.7$ degrees	

$$|1\rangle = |1, 1/2\rangle$$
$$|2\rangle = \cos\theta|0, 1/2\rangle + \sin\theta|1, -1/2\rangle$$
$$|3\rangle = \cos\phi|-1, 1/2\rangle + \sin\phi|0, -1/2\rangle$$
$$|4\rangle = |-1, -1/2\rangle$$
$$|5\rangle = -\sin\phi|-1, 1/2\rangle + \cos\phi|0, -1/2\rangle$$
$$|6\rangle = -\sin\theta|0, 1/2\rangle + \cos\theta|1, -1/2\rangle$$

$$\mathbf{H} = \mathbf{H}_{\text{spinorbit}} + \mathbf{H}_{\text{exchange}}$$
$$\mathbf{H}\text{ex}|m_s\rangle = m_s \text{Hs}|m_s\rangle,\ m_s = \pm 1/2$$
$$\mathbf{H}\text{so}|m_j\rangle = (\zeta/2)|m_j\rangle \text{ for } m_j = 3/2 \text{ and } -\zeta|m_j\rangle \text{ for } m_j = 1/2$$
$$0 \leqslant \sin\theta, \sin\phi, \cos\theta, \cos\phi \leqslant 1$$

$$(2/3)^{1/2} \leqslant \cos\theta \leqslant 1 \qquad 0 \leqslant \theta \leqslant 35.3^\circ$$
$$(1/3)^{1/2} \leqslant \cos\phi \leqslant 1 \qquad 0 \leqslant \phi \leqslant 54.8^\circ$$

$$\tan 2\theta = (2\sqrt{2})/[(2\text{Hs}/\zeta) + 1]$$
$$\tan 2\phi = (2\sqrt{2})/[(2\text{Hs}/\zeta) - 1]$$
$$\langle 1|\text{H}|1\rangle = \text{Hs}/2 + \zeta/2$$
$$\langle 2|\text{H}|2\rangle = \text{Hs}\{\cos^2\theta - 1/2\} + (\zeta/2)\{2\sqrt{2}\cos\theta\sin\theta - \sin^2\theta\}$$
$$\langle 3|\text{H}|3\rangle = \text{Hs}\{\cos^2\phi - 1/2\} + (\zeta/2)\{2\sqrt{2}\cos\phi\sin\phi - \cos^2\phi\}$$
$$\langle 4|\text{H}|4\rangle = -\text{Hs}/2 + \zeta/2$$
$$\langle 5|\text{H}|5\rangle = -\text{Hs}\{\cos^2\phi - 1/2\} - (\zeta/2)\{2\sqrt{2}\cos\phi\sin\phi + \sin^2\phi\}$$
$$\langle 6|\text{H}|6\rangle = -\text{Hs}\{\cos^2\theta - 1/2\} - (\zeta/2)\{2\sqrt{2}\cos\theta\sin\theta + \cos^2\theta\}$$

$$\text{Binding energy shift} = -\langle \text{i}|\text{H}|\text{i}\rangle$$

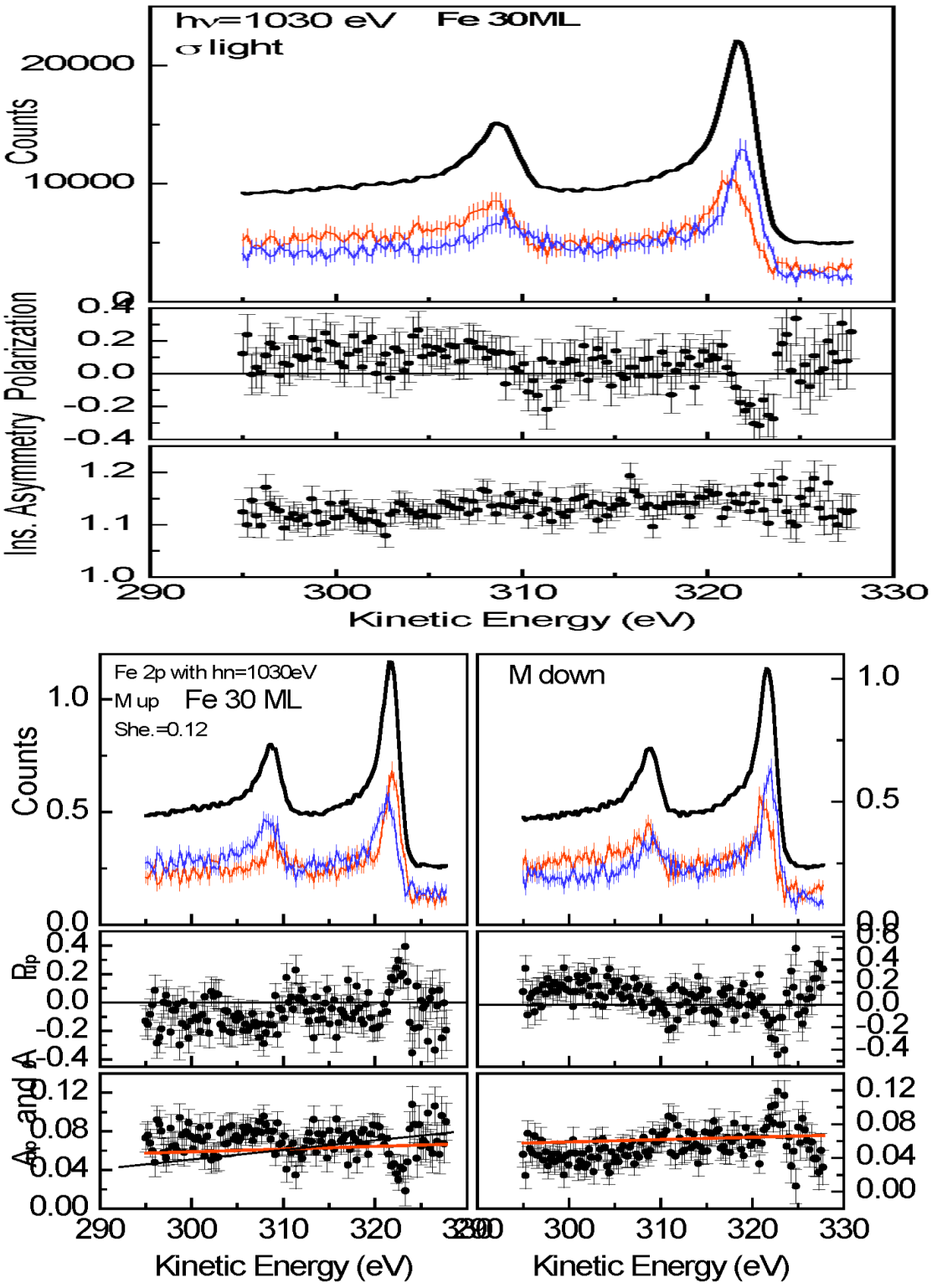
hν=1030 eV Fe 30ML
σ light
Counts
20000
10000
Ins. Asymmetry Polarization
0.4
0.2
0.0
-0.2
-0.4
1.2
1.1
1.0
290
300
310
320
330
Kinetic Energy (eV)
Fe 2p with hn=1030eV
M up Fe 30 ML
She.=0.12
M down
Counts
1.0
0.5
0.0
Rp
0.4
0.2
0.0
-0.2
-0.4
Ap and Am
0.12
0.08
0.04
0.00
290
300
310
320
330
Kinetic Energy (eV)
Kinetic Energy (eV)

Figure 1A

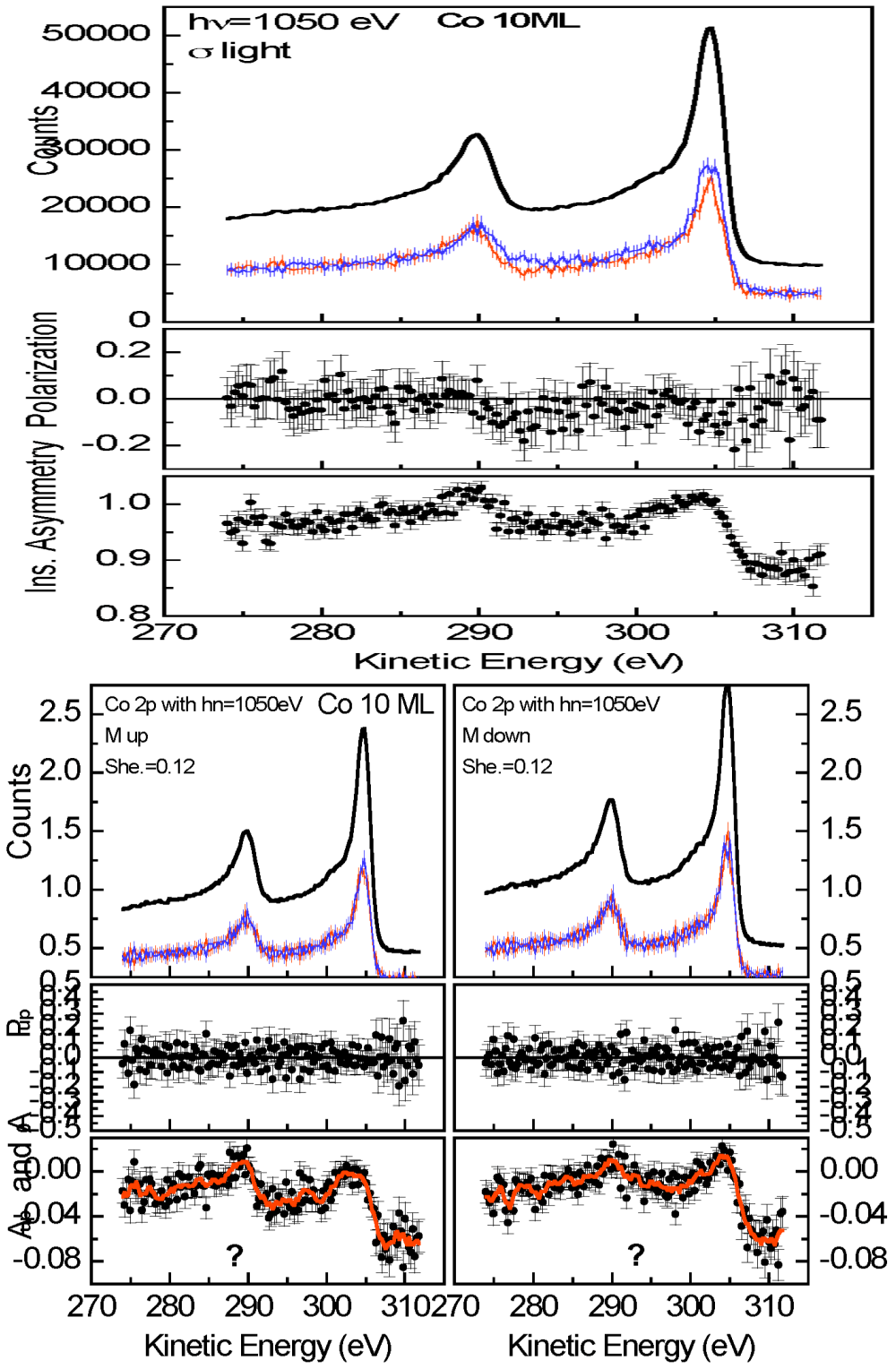
hν=1050 eV Co 10ML
σ light
Counts
Ins. Asymmetry Polarization
Kinetic Energy (eV)
Co 2p with hn=1050eV Co 10 ML
M up
She.=0.12
Co 2p with hn=1050eV
M down
She.=0.12
Counts
Rp
A and Ae
?
?
Kinetic Energy (eV)
Kinetic Energy (eV)

Figure 1B

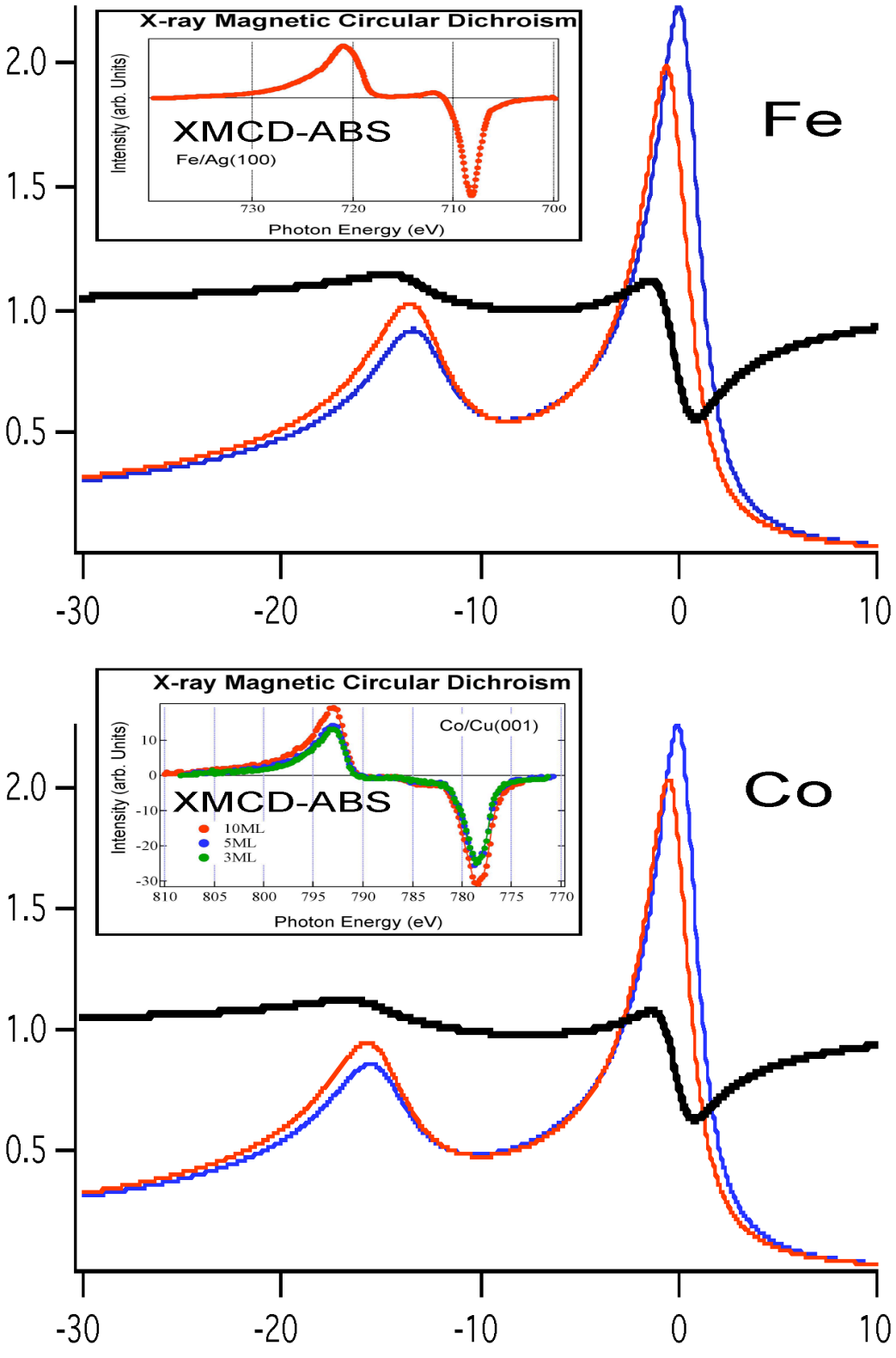
X-ray Magnetic Circular Dichroism
XMCD-ABS
Fe/Ag(100)
Intensity (arb. Units)
Photon Energy (eV)
Fe
X-ray Magnetic Circular Dichroism
XMCD-ABS
Co/Cu(001)
10ML
5ML
3ML
Intensity (arb. Units)
Photon Energy (eV)
Co

Figure 2

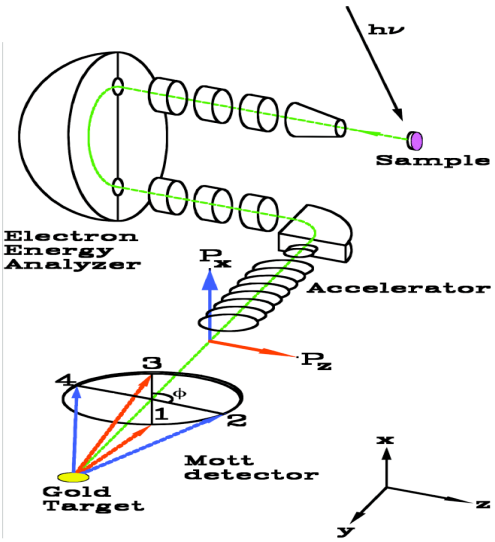
hν
Sample
Electron
Energy
Analyzer
P_x
Accelerator
P_z
3
4
Φ
1
2
Mott
detector
Gold
Target
x
z
y

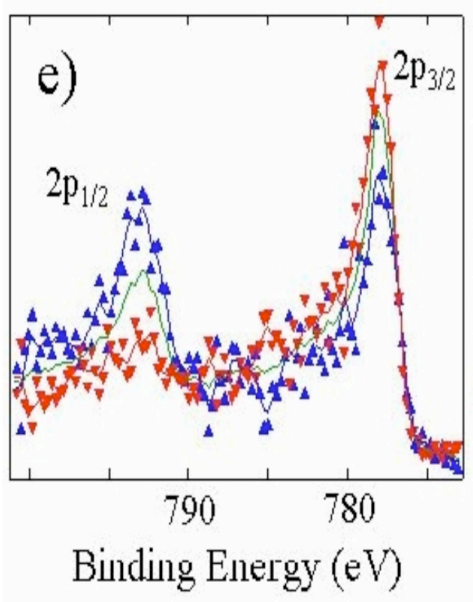
e)
$2p_{3/2}$
$2p_{1/2}$
790
780
Binding Energy (eV)

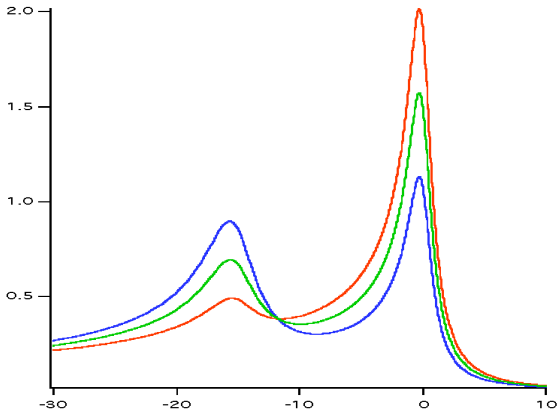
2.0
1.5
1.0
0.5
-30
-20
-10
0
10

Figure 3